Journal of the Less-Common Metals, *136* (1988) 237 - 247

PHASE EQUILIBRIA FOR THE ALUMINUM-RICH REGION OF THE Al–Ru SYSTEM

STEVEN M. ANLAGE*, PHILIP NASH†, RAM RAMACHANDRAN‡ and RICARDO B. SCHWARZ

Center for Materials Science, Los Alamos National Laboratory, Los Alamos, NM 87545 (U.S.A.)

(Received April 27, 1987)

Summary

Measurements by scanning electron microscopy, X-ray diffraction, and thermal analysis show that the aluminum-rich end of the published phase diagram for the Al–Ru system is incorrect. A new phase diagram is proposed for the aluminum-rich end of the diagram. The main differences from the previous diagram are as follows: (1) $Al_{13}Ru_4$ melts peritectically at 1403 °C rather than at 1200 °C, (ii) Al_6Ru melts peritectically at 723 °C rather than congruently at 1340 °C and (iii) we find no evidence for the phase $Al_{12}Ru$, reported earlier. The kinetics of phase formation in this system are discussed with reference to the synthesis of metastable structures such as the icosahedral phase.

1. Introduction

It has recently been found that alloys of aluminum and ruthenium can be crystallized into a metastable icosahedral phase [1, 2]. During our study of the synthesis of the icosahedral phase by mechanical alloying [3] we have found that the published phase diagram for the Al–Ru system [4] is incorrect. The present paper is a study of the aluminum-rich end of this phase diagram.

A tentative phase diagram for the Al–Ru system was proposed by Obrowski [5] in 1963. The six intermetallic compounds identified by Obrowski are on the aluminum-rich side of the diagram. The compound AlRu melts congruently and has a CsCl structure, space group $Pm\bar{3}m$ [4]. Al_3Ru_2 forms peritectically and has the Al_3Ni_2 structure, space group $P\bar{3}m1$.

*Permanent Address: Department of Applied Physics, California Institute of Technology, Pasadena, CA 91125, U.S.A.

†Permanent Address: Metallurgical and Materials Engineering Department, Illinois Institute of Technology, Chicago, IL 60616, U.S.A.

‡Permanent Address: Department of Metallurgical Engineering, Indian Institute of Technology, Kampur-208016, India.

0022-5088/88/$3.50 © Elsevier Sequoia/Printed in The Netherlands

Al_2Ru also forms peritectically, but its structure has not yet been conclusively determined [5]. The crystal structure of $Al_{13}Ru_4$ has been determined by Edshammar [6] to be monoclinic, space group $C2/m$. Obrowski claims that Al_6Ru melts congruently at T_m = 1350 °C. The crystal structure of Al_6Ru is orthorhombic with space group *Cmcm* [7]. Finally, the cubic compound $Al_{12}Ru$ is expected to melt peritectically at T_m = 750 °C [5].

2. Experimental methods

Alloys of $Al_{80}Ru_{20}$ and $Al_{90}Ru_{10}$ were prepared by melting the elements in alumina crucibles. The ruthenium was initially in powder form (purity, 99.95%; Johnson–Matthey). In order to deoxidize this material, the powder was first statically compressed into pellets, 0.375 inches in diameter by 0.1 inches in height. These were placed on a water-cooled "silver boat" enclosed in a high purity argon atmosphere. Induction heating was used to heat simultaneously the ruthenium pellets and a 1 cm^3 piece of high purity zirconium, placed on the silver boat a few inches away. After heating the ruthenium pellet for 45 minutes to slightly below its melting temperature and the zirconium to approximately 700 °C (at this temperature the zirconium is an effective oxygen getter), the ruthenium pellet changed from a dark gray to a shiny gray color. In some cases the edges of the pellets melted. The pellets were then crushed into a coarse powder.

Aluminum (purity, 99.999%; Johnson–Matthey) in the form of rods, 0.25 inches in diameter, was etched in a 90%HNO_3–10%HF solution just prior to alloying. The ruthenium and aluminum were placed in an alumina crucible which was heated in an electrical furnace inside a glove box containing argon. A dynamic purification system circulated the argon at a rate of 40 cubic feet per minute and maintained partial pressures of oxygen and water at levels below 1 ppm.

The alloy casts were slowly cooled in the furnace. As part of another study, some of the ingots were mechanically alloyed (MA) for nine hours in a table-model ball mill (for further details see ref. 8). This produced a fine powder of mostly amorphous alloy with traces of the crystalline phases remaining from the as-cast material.

Thermal analysis of the alloys was performed on a Perkin–Elmer differential thermal analyzer (DTA) for temperatures ranging up to 1400 °C. The DTA was equipped with alumina sample holders and was run in a computer-simulated differential scanning calorimeter (DSC) mode. All runs were performed in a purified argon atmosphere flowing at a rate of 10 - 15 $cm^3\ min^{-1}$.

X-ray diffraction analysis was performed on two instruments. Small quantities of powder were examined by a Debye–Scherrer camera. Larger amounts of powder were used to obtain θ - 2θ diffraction patterns on a Scintag PAD-V diffractometer. Scanning electron micrographs of the as-cast alloys were obtained with a Cam-Scan Series 4 scanning electron microscope

(SEM). Standardless energy dispersive X-ray (EDX) analysis was performed using a Kevex detector through a beryllium window 20 μm thick.

3. Experimental results and discussion

Figure 1 shows the phase diagram of $Al_{1-x}Ru_x$ for $0 < x < 0.25$ and $T < 1400$ °C. The main differences between this diagram and that published previously [4] are (i) $Al_{13}Ru_4$ melts peritectically at approximately 1403 °C rather than at 1200 °C; (ii) Al_6Ru does not melt congruently at 1340 °C, instead it melts peritectically at 723 °C; and (iii) we find no evidence for the phase $Al_{12}Ru$, reported earlier [4].

The evidence for these modifications follows from observations made by SEM/EDX analysis, X-ray diffraction and thermal analysis. These measurements are represented by the solid symbols in Fig. 1 and are discussed below.

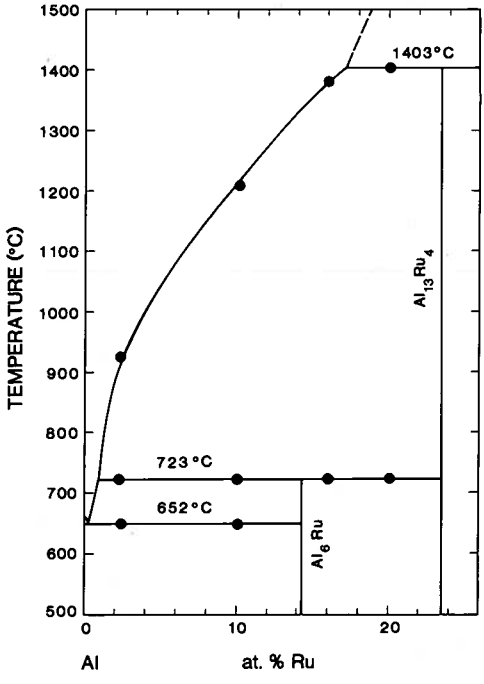

Fig. 1. Phase diagram for the aluminum-rich end of the Al–Ru system; solid symbols represent measured values.

3.1. SEM Observations

An X-ray diffraction pattern of the as-cast $Al_{80}Ru_{20}$ ingot revealed the presence of $Al_{13}Ru_4$, Al_6Ru and aluminum. Figure 2 is an SEM micrograph of this ingot showing a collection of irregularly faceted crystallites of

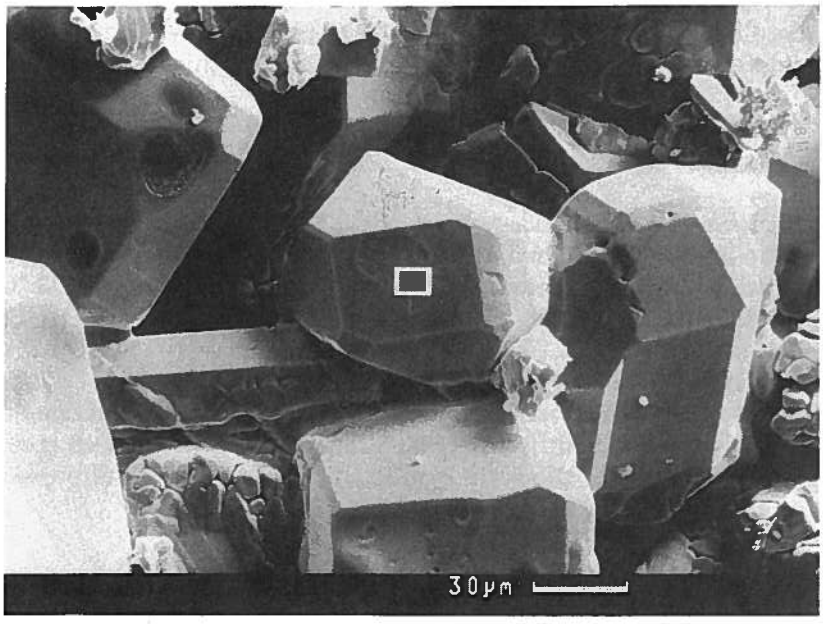

Fig. 2. SEM micrograph showing $Al_{13}Ru_4$ crystals in the as-cast $Al_{80}Ru_{20}$ alloy; the white-framed window shows the area analyzed by EDX.

$Al_{13}Ru_4$. An EDX measurement from the small window near the center of the figure gave the composition $Al_{75.9}Ru_{24.1}$, which is close to the stoichiometric composition $Al_{76.4}Ru_{23.6}$ of $Al_{13}Ru_4$. Measurements from other crystallites yield essentially the same composition.

Figure 3 is an SEM micrograph of the $Al_{80}Ru_{20}$ ingot showing the irregular coral-like morphology of Al_6Ru. This morphology indicates that the growth of the Al_6Ru was *continuous*, rather than along atomic ledges as in the case of $Al_{13}Ru_4$. An EDX measurement from the small window near the center of the figure gave the composition $Al_{84.1}Ru_{15.9}$ which is close to the stoichiometric composition $Al_{85.7}Ru_{14.3}$ of Al_6Ru.

Small droplets of aluminum-rich solution were observed on the surfaces of some of the $Al_{13}Ru_4$ crystallites (see Fig. 2). EDX measurements show that these drops contain 2 - 3 at.% ruthenium. Because, according to Fig. 1, the $Al_{80}Ru_{20}$ alloy should contain only Al_6Ru and $Al_{13}Ru_4$, the presence of aluminum indicates that equilibrium conditions were not achieved during the cooling of the casts. This is more apparent in the SEM micrographs of the $Al_{90}Ru_{10}$ alloy, to be discussed next.

Figure 4 shows the microstructure of $Al_{90}Ru_{10}$ that was melted and cooled in the DSC at a rate of 20 K min^{-1}. The angular crystals are $Al_{13}Ru_4$, as determined by EDX analysis. For this alloy $Al_{13}Ru_4$ is metastable below 723 °C (see Fig. 1). These crystals should have transformed by the peritectic reaction, liquid + $Al_{13}Ru_4 \rightarrow Al_6Ru$. Figure 5 is a higher magnification micrograph showing that the peritectic reaction has not occurred at the boundary between $Al_{13}Ru_4$ (left) and the matrix. Some needle-shaped

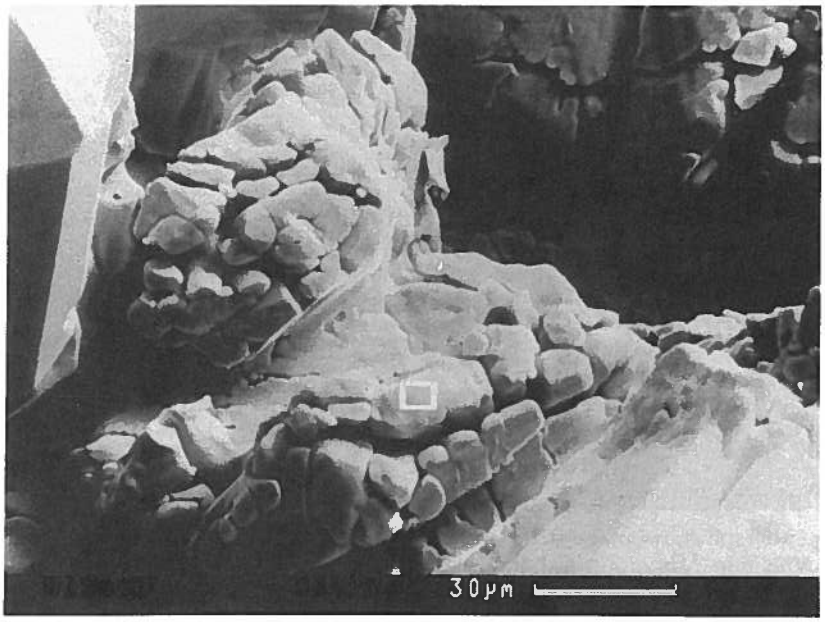

Fig. 3. SEM micrograph showing Al_6Ru crystals in the as-cast $Al_{80}Ru_{20}$ alloy; the white-framed window shows the area analyzed by EDX.

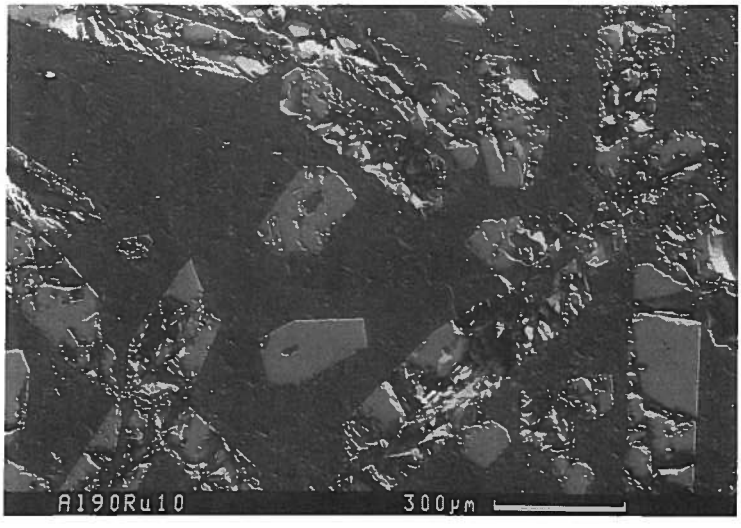

Fig. 4. SEM micrograph showing the structure of $Al_{90}Ru_{10}$ after cooling in the calorimeter at the rate of 20 K min^{-1}; the angular crystals are $Al_{13}Ru_4$ and the matrix is eutectic Al + Al_6Ru.

Al_6Ru crystals (identified by EDX analysis) can be seen in the matrix, but these resulted from eutectic solidification of the liquid at 652 °C.

Figure 6 shows the microstructure of $Al_{90}Ru_{10}$ that was cooled from the melting temperature at a rate of 1 K min^{-1}. This shows that the peri-

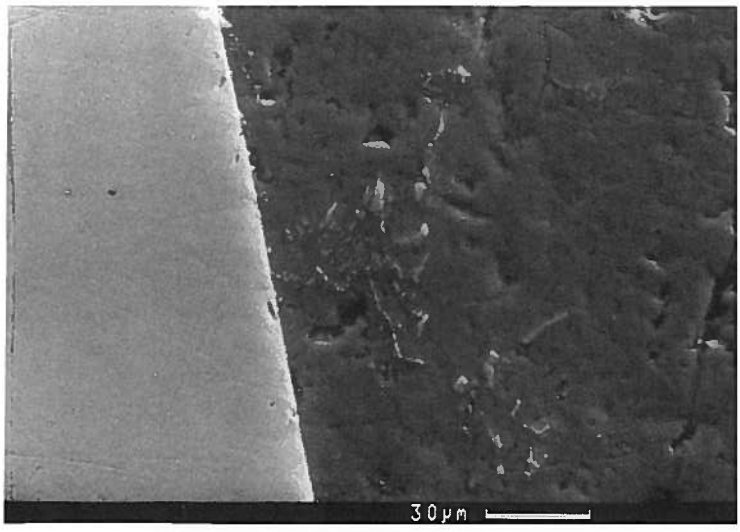

Fig. 5. SEM micrograph showing the structure of $Al_{90}Ru_{10}$ after cooling in the calorimeter at the rate of 20 K min^{-1}, as in Fig. 4, but at higher magnification.

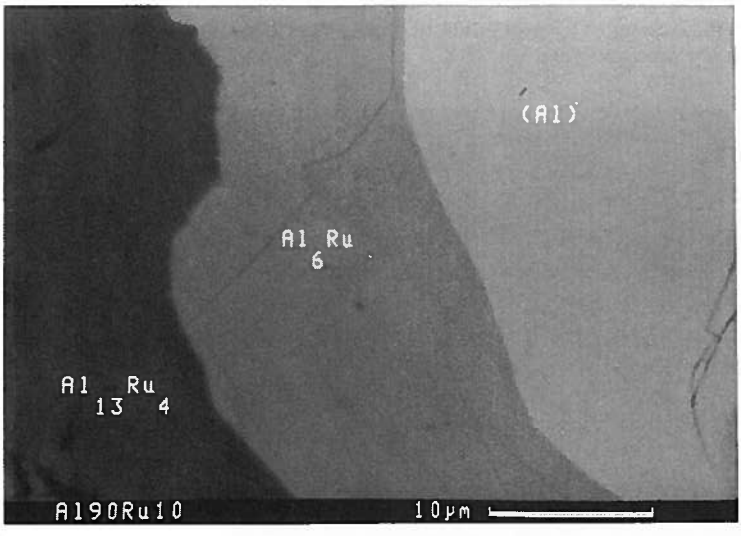

Fig. 6. SEM micrograph showing the structure of $Al_{90}Ru_{10}$ after cooling in the calorimeter at the rate of 1 K min^{-1}; peritectic formation of Al_6Ru is evident at the boundary between $Al_{13}Ru_4$ and the aluminum-rich matrix.

tectic reaction has started at the boundary between $Al_{13}Ru_4$ (left) and the matrix. However, the presence of $Al_{13}Ru_4$ indicates that this reaction has not gone to completion even at this slow cooling rate.

3.2. DSC Measurements

The as-cast material, slowly solidified in an alumina crucible, was chemically heterogeneous on a centimeter-length scale. This material is not

appropriate for DSC studies since the calorimeter employs samples of approximately 60 mg. The as-cast ingots were powdered in either a ceramic mortar and pestle or by mechanical alloying. The resultant powders were also heterogeneous, as shown by X-ray diffraction, but on a much finer scale (of the order of one particle diameter or about 60 μm). Aliquots of the powdered ingots, representative of the average alloy composition, were used for the DSC studies. Approximately fifty milligrams of silver or gold were placed in the reference crucible of the DSC and used to calibrate the temperature and enthalpy scales.

The as-cast $Al_{90}Ru_{10}$ ingot was pulverized in a ceramic pestle and mortar. A Debye–Scherrer X-ray pattern of this material revealed 27 sharp Bragg peaks, all of which were identified as being due to f.c.c. aluminum, Al_6Ru and traces of $Al_{13}Ru_4$. Figure 7(a) shows the DSC trace for the first heat of the pulverized ingot at the heating rate of 20 K min^{-1}. The first endothermic peak, with an onset temperature of 652 °C, corresponds to the eutectic reaction, liquid → (Al) + Al_6Ru. Assuming no $Al_{13}Ru_4$ is present, from the area under the first peak, together with the lever rule applied to the phase diagram in Fig. 1, and the known weights of the $Al_{90}Ru_{10}$ alloy powder and silver in the calorimeter cups, we calculate the enthalpy of fusion of aluminum, $\Delta H^f(Al) = 9.81$ kJ mol^{-1}. This compares favorably with the published value of 10.8 kJ mol^{-1} [9]. The second endothermic peak, with onset temperature 723 °C, corresponds to the peritectic reaction, Al_6Ru → liquid + $Al_{13}Ru_4$. The third peak in Figure 7(a) corresponds to the melting of silver. Because the silver is in the reference crucible of the calorimeter, the melting of the silver appears in the heating runs of Figs. 7 and 8 as an exothermic event. Figure 7(a) does not show the crossing of the liquidus near 1210 °C because, upon approaching the liquidus from below, the amount of $Al_{13}Ru_4$ present decreases smoothly to zero.

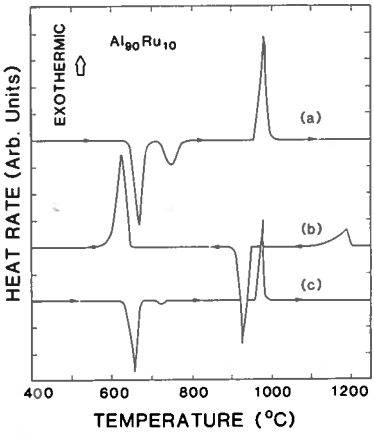

Fig. 7. DSC traces for $Al_{90}Ru_{10}$: (a) heating and (b) cooling at a rate of 20 K min^{-1}, and (c) reheating at a rate of 10 K min^{-1}.

Figure 7(b) shows the DSC trace of the subsequent cooling of the $Al_{90}Ru_{10}$ alloy at 20 K min^{-1}. The first exothermic peak seen on cooling has an onset of 1209 °C and corresponds to the crossing of the liquidus. This crossing is visible on the DSC curve because the liquid undercools slightly before nucleating the $Al_{13}Ru_4$ phase. The second peak in Fig. 7(b), with an onset of 956 °C, results from the solidification of the silver. The peritectic formation of Al_6Ru at approximately 723 °C is absent in Fig. 7(b). In agreement with the SEM observations discussed previously, this indicates that the peritectic formation of Al_6Ru is a very sluggish reaction which is bypassed at the cooling rate of 20 K min^{-1}. The third exothermic peak in Fig. 7(b), with an onset of 652 °C, corresponds to the eutectic solidification of the remaining liquid. There are two possibilities for this reaction

$$\text{liquid} \rightarrow (\text{Al}) + Al_6Ru \tag{1}$$

$$\text{liquid} \rightarrow (\text{Al}) + Al_{13}Ru_4 \tag{2}$$

Equation (2) represents a metastable reaction. The morphology and EDX analysis of the matrix in Fig. 5 shows that the solidification occurs according to eqn. (1). Therefore, the solidification temperature, 652 °C, corresponds to the equilibrium eutectic. Upon further cooling, the liquid composition follows the extrapolation of the liquidus in equilibrium with $Al_{13}Ru_4$ because the peritectic formation of Al_6Ru at 723 °C was bypassed. Thus, at 652 °C the liquid is slightly richer in ruthenium than is the composition of the eutectic of aluminum and Al_6Ru. Hence, upon eutectic solidification, the mass fraction of Al_6Ru formed is greater than that for the equilibrium eutectic composition.

Figure 7(c) is the DSC trace upon reheating the sample of Fig. 7(b) at the rate of 10 K min^{-1}. The first endothermic peak, with onset temperature of 652 °C, is the same as the first peak in Fig. 7(a) and corresponds to the equilibrium eutectic, liquid → (Al) + Al_6Ru. The second small endothermic peak, starting at 723 °C is caused by the peritectic melting of Al_6Ru. The presence of this peak requires further discussion. If upon cooling below 723 °C and reheating, the amount of $Al_{13}Ru_4$ had remained constant, then upon reaching 723 °C all the Al_6Ru would have been dissolved and no peak would have been observed. The presence of a peak at the peritectic temperature of 723 °C indicates that excess Al_6Ru was formed. This may have formed by (i) a reaction in the solid state between aluminum and $Al_{13}Ru_4$ (while cooling the alloy below 652 °C and keeping it at 200 °C for a few hours between the runs of Figs. 7(b) and (c)), and/or (ii) a reaction between liquid (Al) and $Al_{13}Ru_4$ on heating between 652 and 723 °C. We have observed in the DSC traces evidence for both reactions depending on cooling rates and composition. Finally the exothermic peak of Fig. 7(c) corresponds to that in Fig. 7(a).

The ingots of $Al_{80}Ru_{20}$ were homogenized by mechanical alloying. The MA powder contains metastable phases, mainly amorphous Al_xRu_{1-x} alloy. Consequently, several exothermic (irreversible) peaks appear on the

DSC trace during the initial heating of the MA powders, denoting transformations of the amorphous phase into crystalline phases. These transformations will not be discussed here. In order to eliminate the amorphous phase in the MA powder, the samples were heated to temperatures between 800 and 1400 °C and cooled in the calorimeter. All subsequent DSC measurements were performed on the material which remained undisturbed in the apparatus. An X-ray diffraction pattern of the annealed MA powder revealed approximately 100 Bragg peaks, all of which could be indexed to the known patterns of aluminum, $Al_{13}Ru_4$ and Al_6Ru.

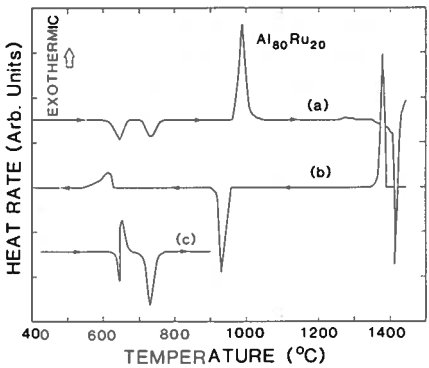

Fig. 8. DSC traces for $Al_{80}Ru_{20}$: (a) heating and (b) cooling at a rate of 20 K min^{-1} after preannealing above 1403 °C; and (c) heating at a rate of 25 K min^{-1} after preannealing to 880 °C.

Figure 8(a) shows a typical heating DSC trace for $Al_{80}Ru_{20}$ powder at 20 K min^{-1}. Before this run, the powder was heated in the calorimeter to a temperature above 1403 °C, sufficient to melt the $Al_{13}Ru_4$ phase present in the powder. If upon cooling, the alloy had followed the equilibrium phase diagram, it would have consisted only of Al_6Ru and $Al_{13}Ru_4$ below 723 °C. The presence of the eutectic endotherm at 652 °C in Fig. 8(a) is in agreement with the results for the $Al_{90}Ru_{10}$ alloy, discussed previously, which show that on cooling the Al_6Ru phase has difficulty in nucleating peritectically at 723 °C and instead forms eutectically at 652 °C, as clearly shown in Figs. 7(b) and 8(b). The second endothermic peak in Fig. 8(a) corresponds to the peritectic melting of Al_6Ru. The third peak corresponds to the melting of the silver. The last endothermic peak in Fig. 8(a) corresponds to the peritectic melting of $Al_{13}Ru_4$.

Figure 8(b) is the DSC trace during cooling at 20 K min^{-1}, following the heating run of Fig. 8(a). The peaks with onsets near 1400 and 960 °C correspond to those of opposite sign in Fig. 8(a). As in Fig. 7(b), the peritectic solidification of Al_6Ru around 720 °C is bypassed during cooling at 20 °K min^{-1}. The exothermic peak starting at 652 °C is caused by the eutectic solidification of the remaining liquid.

Figure 8(c) is a DSC trace at the heating rate of 25 K min^{-1} for another aliquot of the MA $Al_{80}Ru_{20}$ powder. As for the DSC run in Fig. 8(a), the

powder was first annealed in the calorimeter to remove the amorphous phase formed by MA. However, the pre-anneal of the powder in Fig. 8(c) differed from that for the powder in Fig. 8(a) in that the maximum temperature was about 880 °C, well below that necessary to melt the $Al_{13}Ru_4$ phase. This anneal is sufficient to crystallize the $Al_{13}Ru_4$ but in a finely dispersed form. Upon cooling this powder, the peritectic crystallization of Al_6Ru at 723 °C is bypassed. Below 652 °C, Al_6Ru forms eutectically. Thus the $Al_{13}Ru_4$, aluminum and Al_6Ru phases remain finely dispersed within each powder particle, creating large interfacial areas. Hence, on reheating to 652 °C, the Al–Al_6Ru eutectic melts and the liquid, in close contact with the $Al_{13}Ru_4$, reacts with it to form Al_6Ru. This explains the endothermic–exothermic doublet at the beginning of Fig. 8(c). This doublet is not seen in Fig. 8(a), nor in Fig. 7(c), because in both cases the $Al_{13}Ru_4$ crystals nucleated at small undercoolings, giving rise to relatively large $Al_{13}Ru_4$ crystals (see Fig. 4) with a relatively small Al–$Al_{13}Ru_4$ interfacial area. Upon heating these crystals and melting the aluminum, the reaction, liquid + $Al_{13}Ru_4 \rightarrow Al_6Ru$, gives rise to a small exothermic peak that cannot be resolved since it is superimposed on the much larger endothermic reaction, Al + $Al_6Ru \rightarrow$ liquid. Similar DSC measurements were obtained for $Al_{98}Ru_2$ and $Al_{84}Ru_{16}$ alloys. These measurements allowed us to map out the equilibrium phase diagram of Fig. 1.

4. Conclusions

The phase diagram of Al–Ru shown in Fig. 1 was deduced from X-ray diffraction analysis, microstructure characterization and calorimetry. The solid symbols in this figure are measured values. The main differences between Fig. 1 and the phase diagram proposed by Obrowski [5] are (i) $Al_{13}Ru_4$ melts peritectically at 1403 °C rather than at 1200 °C, (ii) Al_6Ru melts peritectically at 723 °C rather than congruently at 1340 °C, and (iii) we find no evidence for the phase $Al_{12}Ru$.

We have found that in the Al–Ru system the peritectic formation of Al_6Ru is bypassed even at cooling rates as low as 20 K min^{-1}. Therefore, icosahedral phase (IP) formation by rapid solidification has no kinetic competition from the growth of Al_6Ru. The composition of the IP of Al–Ru appears to be lower in ruthenium than that of $Al_{13}Ru_4$. Follstaedt and Knapp [10] have reported forming a single IP alloy by ion mixing at the composition $Al_{84}Ru_{16}$. Anlage *et al.* [11] report that the composition of the IP formed by the rapid solidification of melt in a piston and anvil is approximately $Al_{81}Al_{19}$. Furthermore, IP formation by rapid solidification is obtained for the broad range $Al_{97.6}Ru_{2.4}$ to $Al_{76.5}Ru_{23.5}$. However, even at the high cooling rates achieved in the piston and anvil method there is sufficient kinetic competition from partitionless crystallization of (Al) and $Al_{13}Ru_4$ to prevent the formation of a single icosahedral phase.

Icosahedral phase formation has been observed in several Al–transition metal (TM) alloy systems in the region of 20 at.% solute [1]. In this compo-

sition region, all systems have in common (i) a rapidly falling liquidus, (ii) the peritectic formation of several intermetallic compounds, (iii) virtually no terminal solubility and (iv) a metallic radius (coordination number 12) ratio between the aluminum and the TM of approximately 1.05 which is appropriate for local icosahedral packing. These empirical observations may assist in the search for new icosahedral-phase forming systems. Examples of systems not containing aluminum that exhibit similar features, and therefore may be good candidates for icosahedral phase formation, are the gallium-rich end of the Ga–Mn and Ga–Pd systems and the zinc-rich end of the Zn–Mn system.

Acknowledgments

S.M.A., P.N. and R.R. acknowledge the support and hospitality of the Center for Materials Science at Los Alamos National Laboratory. Also, S.M.A. acknowledges support by Eastman Kodak and I.B.M. pre-doctoral fellowships.

References

1 P. Bancel and P. A. Heiney, *J. Phys. (Paris), Colloq., 47* (3) (1986) 341.
2 D. M. Follstaedt and J. A. Knapp, *Mater. Sci. Eng., 90* (1987) 1.
3 S. M. Anlage, R. Ramachandran and R. B. Schwarz, in preparation (1987).
4 F. Shunk, *Constitution of Binary Alloys, Second Supplement*, McGraw–Hill, New York, 1969, p. 40.
5 W. Obrowski, *Metall (Berlin), 17* (1963) 108.
6 L. Edshammar, *Acta Chem. Scand., 19* (1965) 2124.
7 L. Edshammar, *Acta Chem. Scand., 22* (1968) 2374.
8 R. B. Schwarz, R. R. Petrich and C. K. Saw, *J. Non-Cryst. Solids, 76* (1985) 281.
9 E. A. Brandes, *Smithells Metals Reference Book*, Butterworths, London, 6th edn., 1983, p. 8 - 1.
10 D. M. Follstaedt and J. A. Knapp, *Mater. Sci. Eng., 90* (1987) 1.
11 S. M. Anlage, B. Fultz and K. M. Krishnan, submitted to *J. Mater. Res.* (1987).